

Heat transport and pedestal structure of H-mode in the variation of current density profiles in JT-60U

H. Urano, Y. Sakamoto, T. Suzuki, T. Fujita, K. Kamiya, A. Isayama, Y. Kamada,
H. Takenaga, N. Oyama, G. Matsunaga, S. Ide, Y. Idomura and JT-60 Team

Japan Atomic Energy Agency, Naka Fusion Institute, Naka, Ibaraki 311-0193 Japan
e-mail contact of main author: urano.hajime@jaea.go.jp

Abstract. H-modes operated at higher I_i with the current ramp down have shown higher energy confinement with higher density in JT-60U. The H-factor evaluated for the core plasma depends strongly on I_i with the relation of $H_{89\text{core}} \propto I_i^{0.77}$ for the case without sawtooth activities. Center peaked profiles of electron density and electron temperature are obtained in high I_i H-modes. While the peripheral current density profiles are largely modified by the current ramp, the pedestal pressure is not significantly changed. The enhanced energy confinement in high I_i H-modes is attributed to the core improvement with the peaked profiles of electron density and electron temperature while no explicit difference in pedestal profile is observed. The electron heat diffusivity is reduced at the plasma core in high I_i case, resulting in the center peaked T_e profile while the T_i profiles are approximately unchanged.

In addition, the characteristics of the spatial width Δ_{ped} of the H-mode pedestal are investigated in hydrogen and deuterium plasmas in JT-60U. Similar edge profiles of the ion temperature are obtained for both cases while ρ^*_{pol} is not fixed but differs by a factor of ~ 1.4 (which is the square root of the mass ratio). This result suggests a weak dependence of Δ_{ped} on ρ^*_{pol} . Based on these dimensionless parameter scans, the scaling was evaluated as $\Delta_{\text{ped}} \propto a\rho^*_{\text{pol}}{}^{0.2}\beta_{\text{pol}}{}^{0.5}$.

1. Introduction

Tokamaks are a system in which magnetized plasmas are confined by a poloidal magnetic field generated by the plasma current I_p in combination with the toroidal magnetic field. It has been therefore presumed that the heat transport in the plasma core could depend implicitly or explicitly on the current density profile $j(r)$. Therefore, understanding the response of temperature profiles to variations in current density profile is indispensable for predicting a future fusion reactor. In this study, conducting the I_p ramp experiments in JT-60U, the heat transport and edge pedestal structure in the variation of the current ramp up and down discharges are examined.

In H-mode plasmas, the edge pedestal structure determines the boundary condition of the heat transport of the plasma core [1]. Therefore, it is of primary importance to understand the physical processes determining the edge pedestal structure. However, the dependence of the spatial width Δ_{ped} of the edge transport barrier on local parameters is not clearly known. In this study, focusing on the poloidal dimensionless parameters in the poloidal system determined by I_p , the dependence of Δ_{ped} on ρ^*_{pol} and β_{pol} is examined by conducting dedicated mass scan experiments using hydrogen and deuterium plasmas.

2. Current ramp experiment on ELMy H-mode plasmas

Fig. 1 shows the waveforms of a pair of the plasma current (I_p) ramp discharges where the positive ion-based NB of 8.8MW is injected. In these two discharges, the operational conditions are the same except I_p ramping phase. The experiments were performed at $I_p = 1.15\text{MA}$ and $B_T = 2.6\text{T}$. The safety factor at 95% flux surface q_{95} was fixed at ~ 4.1 . The elongation is $\kappa \sim 1.4$ and the triangularity is $\delta \sim 0.35$. As shown in Fig. 1(a), in case of the I_p ramp up, I_p is raised from 0.90MA to 1.15MA, while I_p is decreased from 1.40MA to 1.15MA in case of the I_p ramp down. The I_p ramp rate is $dI_p/dt = 550\text{kA/s}$ for both cases. Comparing

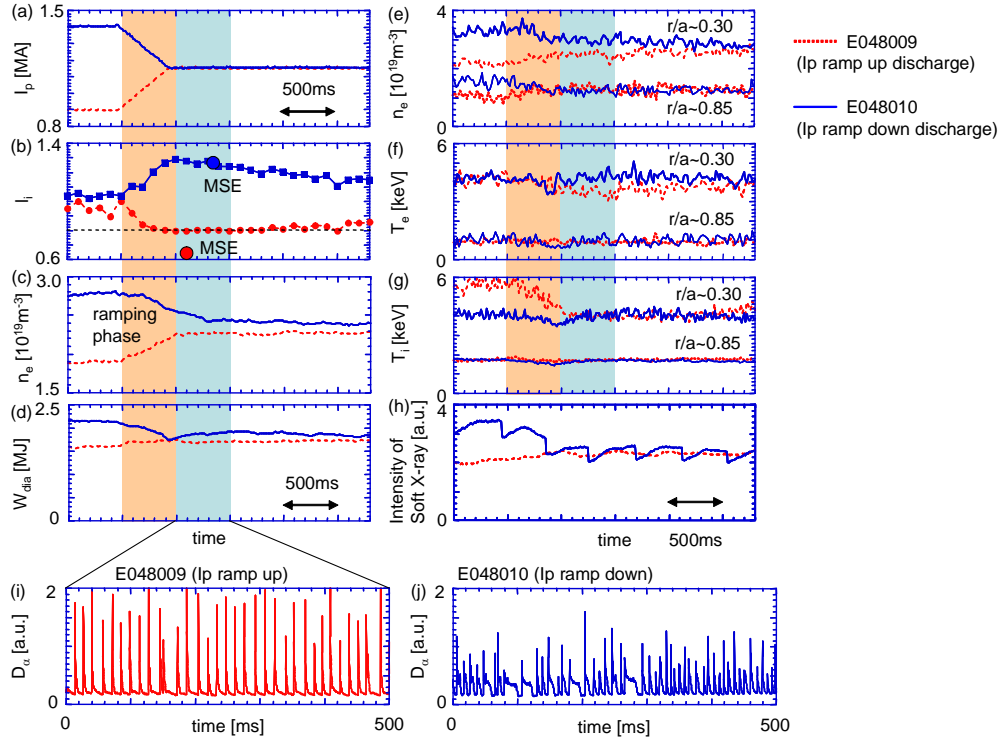


FIG. 1. Temporal evolution of plasma parameters for the cases of the current ramp up and down discharges; (a) I_p : plasma current, (b) l_i : internal inductance, (c) n_e : line-averaged electron density, (d) stored energy measured with a diamagnetic loop, (e) electron density, (f) electron temperature and (g) ion temperature measured at $r/a=0.2$ and 0.8 , (h) intensity of soft X-ray at the plasma center. Broken and solid line indicates the I_p ramp up and down discharges, respectively. The intensity of D_α emission is also shown for the cases of (i) I_p ramp up and (j) down discharges.

the ELMy H-mode plasmas after the I_p ramp phase, the influence of the current density profile on the heat transport can be examined in a situation where the current density profile is explicitly varied while keeping the I_p value fixed at 1.15MA. In this series of experiments, the plasma equilibrium is reconstructed using the MSE measurement.

Fig. 1(b) shows the time evolution of the internal inductance l_i . After the I_p ramp up and down phase, the l_i becomes smaller to 0.6 and larger to 1.3, respectively. Compared to the lower l_i case, the line-averaged density measured with the FIR interferometer becomes higher by $\sim 8\%$ at higher l_i case (see Fig. 1(c)), and the stored energy W_{dia} measured with a diamagnetic loop is also higher by $\sim 12\%$ (see Fig. 1(d)). As shown in Figs. 1(e) and (f), the n_e and T_e profiles tend to be peaked at the center at higher l_i while the T_i profile is not clearly changed (see Fig. 1(g)). The n_e , T_e and T_i values at the H-mode pedestal ($r/a \sim 0.85$) are almost identical. Fig. 1(h) shows the intensity of Soft X-ray measured at the plasma center. In case of the I_p ramp down, the deeply penetrated current density profile induces the sawtooth activity with the frequency $f_{\text{SW}} \sim 2.5\text{Hz}$. The inversion radius of this sawtooth activity is $r/a \sim 0.2$. Figs. 1(i) and (j) show the intensity of the D_α emission in the outer divertor region. In spite of the changes in the edge pedestal parameters, such as n_e , T_e and T_i , are small, a clear difference is observed in ELM activity. The ELM frequency f_{ELM} of $\sim 140\text{Hz}$ at higher l_i case is larger by a factor of 2 than f_{ELM} of $\sim 70\text{Hz}$ at lower l_i case.

The result obtained in this current ramp experiment indicates that the increase of W_{dia} at higher l_i is attributed mainly to the peaked profiles of n_e and T_e while the pedestal pressure p_{ped} is not clearly changed. On the other hand, the T_i profile is not significantly changed so that a constant scale length of dT_i/dr is sustained at which the profile is determined by the pedestal temperature.

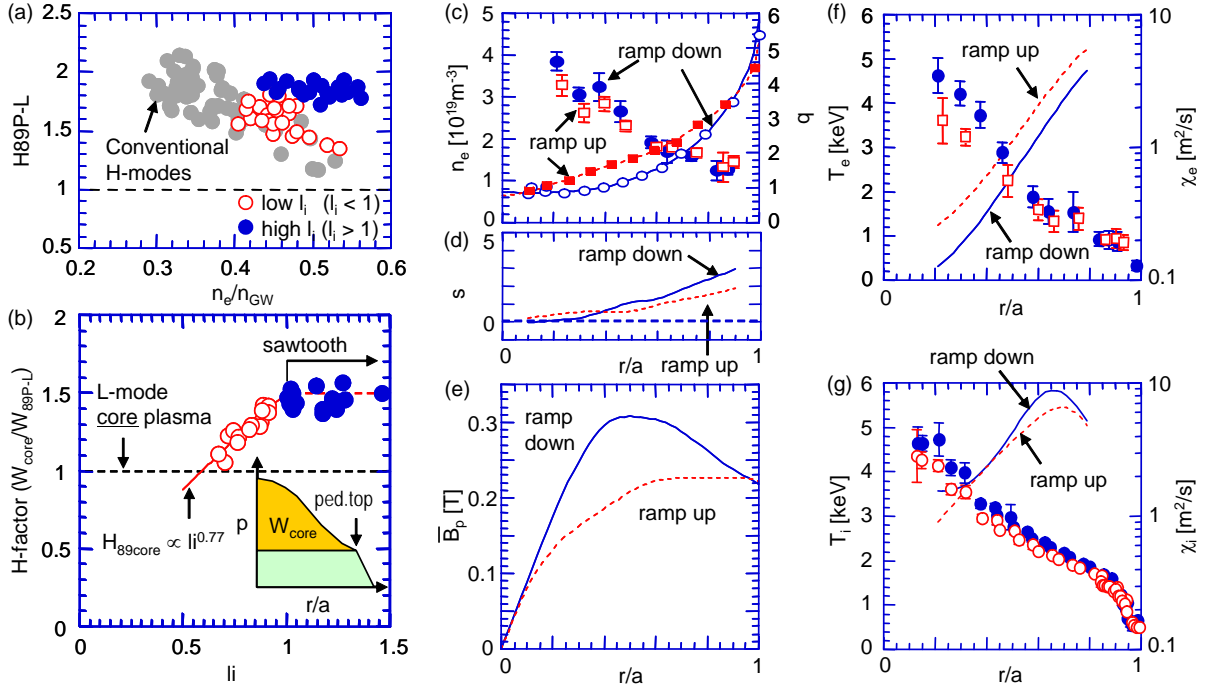


FIG. 2. (a) The H-factor as a function of n_e/n_{GW} . (b) Relation between the core H-factor for the H-mode plasmas and l_i . Spatial profiles of (c) n_e , q , (d) the magnetic shear s , (e) the poloidal magnetic field averaged over the poloidal angle, (f) T_e , χ_e , (g) T_i and χ_i . The profiles are taken for the cases of low ($l_i \sim 0.7$) and high l_i (~ 1.3) at $I_p = 1.15\text{MA}$ and $P_{abs} = 7\text{MW}$.

3. Reduction of heat transport in high l_i H-mode plasmas

In conventional H-mode plasmas, the energy confinement degrades in many cases with density through the p_{ped} limited by the existence of ELM and the profile resilience [1]. However, as described in Sec. 2, when the l_i value becomes larger, the electron density tends to increase accompanied by the increase of the plasma stored energy. Fig. 2(a) shows the relation between the H-factor and the n_e normalized to the Greenwald density limit n_{GW} . Compared to the lower l_i cases where the H-factor of 1.3-1.8 at $n_e/n_{GW} = 0.40$ -0.55, higher density of $n_e/n_{GW} = 0.44$ -0.57 is reached without the deterioration of the energy confinement ($H_{89P-L} = 1.8$ -2.0). In the previous study on the L-mode plasmas, it was shown that the energy confinement depends strongly on the l_i value as $H_{89P-L} \propto l_i$ [2]. In order to compare with the case of L-mode, the H-factor evaluated for the core plasma of H-mode (H_{89core}) as a function of l_i is shown in Fig. 2(b). In this figure, H_{89core} is defined as W_{core}/W_{89P-L} where W_{core} denotes the core stored energy in H-mode plasmas and W_{89P-L} is the stored energy estimated from the ITER89P L-mode scaling. Since the H-mode plasmas are accompanied by the pedestal structure, the dependence of the energy confinement on l_i should be analyzed with subtracting the energy given by the H-mode pedestal structure. In case of $l_i < 1$, the H-factor for the core plasma depends strongly on l_i with the relation of $H_{89core} \propto l_i^{0.77}$. This relation is similar to L-mode plasmas [2]. However, at $l_i > 1$, the existence of strong sawtooth prevents from the increase of the core H-factor at higher l_i regime ($H_{89core} \sim 1.5$ at $l_i > 1$). This tendency is also seen in the case of L-mode plasmas.

Let us then compare the spatial profiles of n_e , T_e and T_i between the cases with low and high l_i at P_{NBI} of 8.8MW ($P_{abs} \sim 7\text{MW}$). The l_i values are 0.7 and 1.3 for the cases of the current ramp up and down discharges, respectively. Although the q_{95} values (~ 4.1) are almost the same, the core q profile differs explicitly by adopting the current ramp technique. Figs.

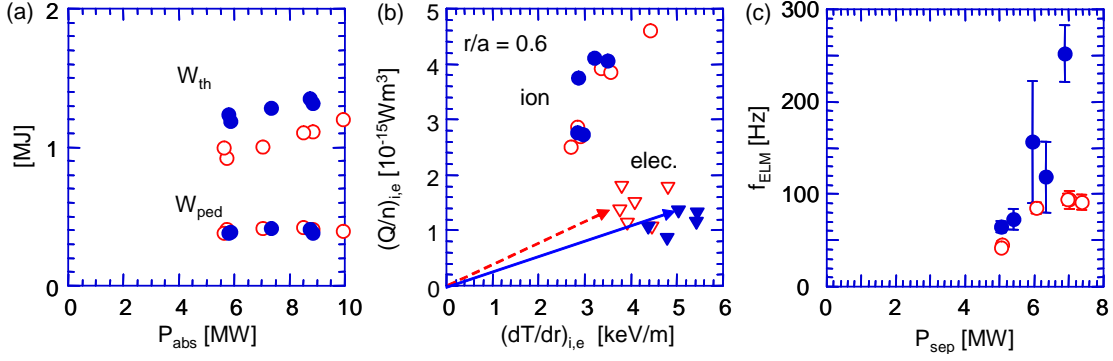


FIG. 3. (a) Thermal and pedestal stored energy as a function of P_{abs} for the cases of low and high l_i H-modes. (b) The $(Q/n, dT/dr)$ diagram for ions and electrons evaluated at $r/a = 0.6$ in a series of power scan. (c) Dependence of ELM frequency on the power crossing the separatrix.

2(d) and (e) show the spatial profiles of the magnetic shear s and the poloidal magnetic field strength averaged over the poloidal angle. In case of high l_i H-mode, the increased central current density enhances the core B_p value particularly around $r/a \sim 0.5$ at which B_p are 0.21T in low l_i case and 0.31T in high l_i case (see Fig. 2(e)). The magnetic shear becomes gradually stronger in the plasma edge region ($r/a \geq 0.6$). In high l_i case, the sawtooth events of 2.5Hz appear with the inversion radius of $\sim 0.2a$. Then, one can find that increased density at high l_i is attributed to the center peaked n_e profile (see Fig. 2(c)). In this series of experiments, the p_{ped} remains almost constant in the variation of $j(r)$. Therefore, the pedestal profiles of T_i are also similar. The T_e profile becomes peaked at the center in high l_i H-mode (see Fig. 2(f)) while the change in the T_i profile is small (see Fig. 2(g)). The electron heat diffusivity χ_e is reduced in the core plasma in high l_i case (see Fig. 2(f)), resulting in the center peaked T_e profile. In case of high l_i H-mode, because of the increased density, the heat deposition of the fast ions becomes broader and its spatial peak shifts towards the edge. The ion conductive heat fluxes at $r/a = 0.6$ for the cases of low and high l_i H-modes are $3.7 \times 10^4 \text{W/m}^2$ and $4.8 \times 10^4 \text{W/m}^2$, respectively. A slight increase of the ion heat diffusivity χ_i corresponds to this difference of the ion conductive heat flux. That is why the influence of the current density profile on the ion heat transport is not as strong as that on the electron heat transport.

In the H-mode plasmas, when the heat flux is increased, the response of dT_i/dr is gradually desensitized and saturated eventually. This ‘power degradation’ seen in the standard H-mode plasmas accompanies in many cases the saturated core temperature gradient. In order to evaluate the level of the achievable temperature gradient depending on the current density profile, the power scan was conducted from $P_{abs} = 6\text{MW}$ to 10MW . Fig. 3(a) shows the thermal stored energy W_{th} and the pedestal energy W_{ped} as a function of P_{abs} . While W_{th} increases gradually with P_{abs} for both cases of low ($l_i = 0.6-0.8$) and high l_i H-modes ($l_i = 1.3-1.4$), it is found at higher l_i that larger W_{th} is obtained at a given P_{abs} . On the other hand, as expected from the result shown in Sec. 2, no clear difference in W_{ped} is observed. From this figure, one can find that the increase of W_{th} at higher l_i is attributed to the energy confinement improvement in the core plasma. Heat transport driven by the temperature gradient can be characterized in a diagram of the heat flux divided by the density Q/n and the temperature gradient dT/dr . Fig. 2(b) shows the $(Q/n, dT/dr)$ diagram for ions and electrons evaluated at $r/a = 0.6$ in a series of power scan. In this diagram, the angle θ formed between the horizontal axis and a straight line which passes through both the data and the origin of the coordinates indicates the heat diffusivity χ ($= \tan^{-1}\theta$). For the ions, as the heat flux is increased, χ_i becomes larger. However, the changes in χ_i in the power scan are similar between the low and high l_i cases. On the contrary to the ions, dT_e/dr becomes stronger at a given heat flux, resulting in the reduction in χ_e although the data are somewhat scattered. Fig. 3(c) shows the

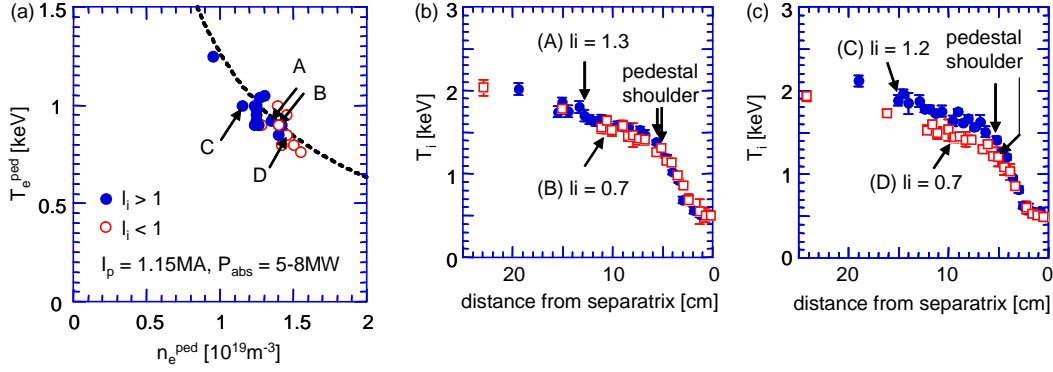


FIG. 4. (a) The pedestal n - T diagram for the cases of low and high l_i H-modes at $I_p = 1.15\text{MA}$. (b) The edge T_i profiles for the case of the similar edge density. (c) The edge T_i profiles for the case of a different edge density. Open squares and closed circles indicate the H-mode plasmas at low and high l_i , respectively.

f_{ELM} as a function of the power crossing the separatrix P_{sep} . As described in Sec. 2, f_{ELM} at higher l_i becomes higher at a given P_{sep} . The I_p ramp primarily changes the edge current density profile. It is considered that the change in the edge current density profile affects strongly the ELM activity. The edge pedestal pressure is insensitive to the edge current density as seen in Fig 3(a).

Fig. 4(a) shows the edge pedestal n_e - T_e diagram for the I_p ramp experiments at $I_p = 1.15\text{MA}$ and $P_{\text{abs}} = 5\text{-}8\text{MW}$. One can find that the pedestal pressure remains almost constant in the variation of the current density profile. Although the data is not systematically separated by l_i , higher l_i H-mode tends to have relatively lower pedestal density. When the current density is penetrated to the center, the density profile is peaked at the center. This might cause the reduction of the edge density. Since the achievable pedestal pressure is almost constant at a given I_p , the pedestal temperature becomes higher when the edge density is decreased in higher l_i plasmas. Fig. 4(b) shows the edge T_i profiles for the case of a similar pedestal density ($n_e^{\text{ped}} \sim 1.4 \times 10^{19} \text{m}^{-3}$ at $P_{\text{abs}} \sim 7\text{MW}$) indicated as (A) and (B) in Fig. 4(a). Then, the edge T_i profiles are also similar. Fig. 4(c) shows the edge T_i profiles for the cases of low and high pedestal densities ($n_e^{\text{ped}} \sim 1.1 \times 10^{19} \text{m}^{-3}$ and $1.4 \times 10^{19} \text{m}^{-3}$ at $P_{\text{abs}} \sim 7\text{MW}$) indicated as (C) and (D) in Fig. 4(a). In the case of higher l_i plasma, higher pedestal temperature of $T_i^{\text{ped}} \sim 1.4\text{keV}$ is obtained by the reduced edge density while the pedestal pressure is almost the same. Note that this experiment is conducted so that the current density profile is changed but the I_p is fixed. In other words, the edge B_p values are almost the same as shown in Fig. 2(e). This result suggests that the pedestal structure such as the spatial width of the edge transport barrier is determined by the edge B_p value.

4. Spatial width of H-mode edge pedestal

A variety of empirical scalings of Δ_{ped} in the H-mode plasmas have been proposed [3-6]. However, these scalings vary from machine to machine, in which ρ_{pol}^* and β_{pol} are intermingled. This disagreement of the scalings can be caused by the existing edge stability boundary for ELMs. In this region, ρ_{pol}^* and β_{pol} are strongly linked and thus hard to separate out. To distinguish these variables, a pair of experiments in hydrogen and deuterium plasmas are conducted [7]. An explicit difference between ρ_{pol}^* and β_{pol} is the mass dependence of ρ_{pol}^* ($\propto m^{0.5}$) in contrast to no mass dependence in β_{pol} .

The experiments were carried out at fixed $I_p = 1.08\text{MA}$, $B_T = 2.4\text{T}$, $\kappa = 1.4$, $\delta = 0.35$ for deuterium and hydrogen discharges. Figs. 5(a), (b) and (c) show the spatial profiles of n_e , T_e and T_i for these two cases, respectively. By using a power scan during a discharge,

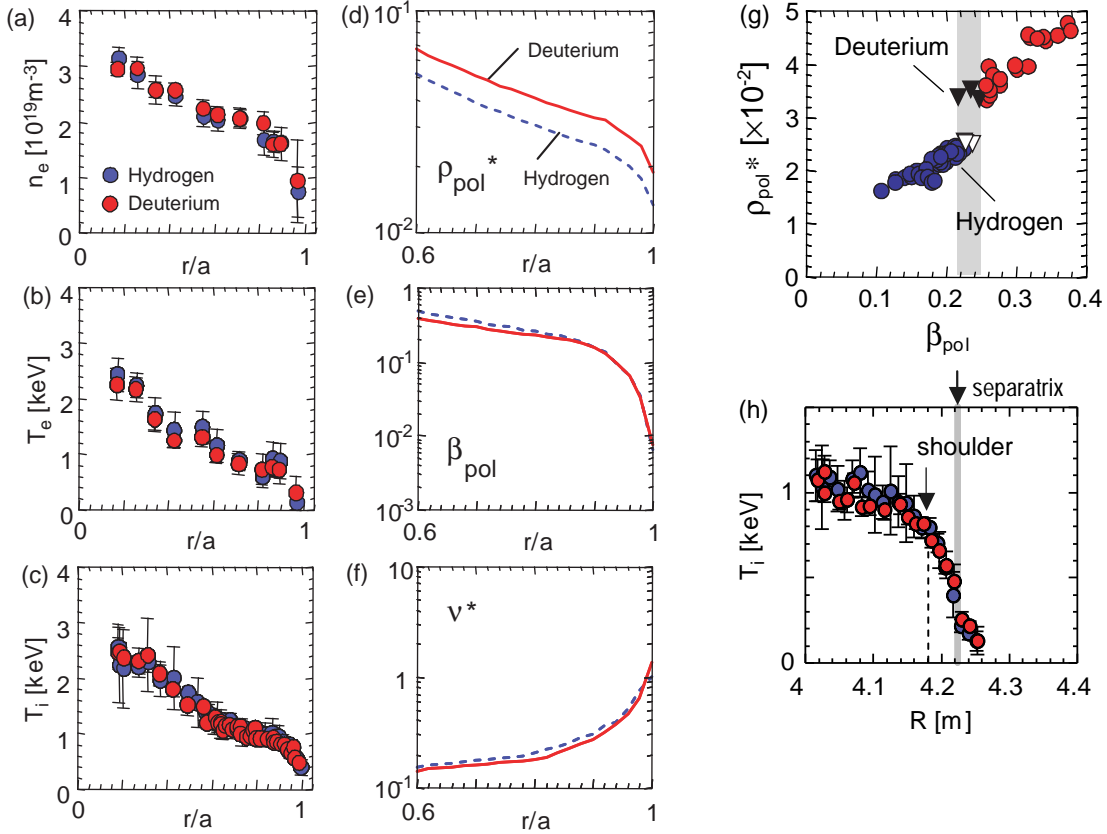


FIG. 5. Radial profiles of (a) n_e , (b) T_e , (c) T_i , (d) ρ_{pol}^* , (e) β_{pol} and (f) v^* for the cases of hydrogen and deuterium discharges. Blue circles and broken curves indicate the hydrogen plasmas. Red circles and solid curves indicate the deuterium plasmas. (g) Data area in β_{pol} - ρ_{pol}^* space of the experiments. Closed and open inverse triangles indicate the deuterium and hydrogen plasmas at a given β_{pol} (~ 0.23), respectively. (h) Pedestal T_i profiles for the deuterium (Red circles) and hydrogen plasmas (blue circles) at the same β_{pol} and v^* .

temperature profiles can be obtained so that the profiles of β_{pol} and v^* are matched. The required power in the hydrogen plasma is ~ 2 times larger than that in deuterium plasma to sustain the same β_{pol} at the plasma edge. Figs. 5(d), (e) and (f) show the spatial profiles of ρ_{pol}^* and β_{pol} and v^* for these two cases. Profiles of β_{pol} and v^* are both well matched across the peripheral plasma. The ρ_{pol}^* profile for the H-mode edge pedestal is not fixed but differs by the factor of ~ 1.4 (which is the square root of the mass ratio). This separation of the link between β_{pol} and ρ_{pol}^* is possible by introducing hydrogen and deuterium plasmas as shown in Fig. 5(g). A strong correlation between β_{pol} and ρ_{pol}^* is seen in each species. At $\beta_{pol} \sim 0.23$ in the pedestal region, the ρ_{pol}^* scan is possible comparing hydrogen and deuterium plasmas. Shown in Fig. 5(h) is the spatial profiles of T_i enlarged to the peripheral region of Fig. 5(g). One can find that the edge T_i profiles are similar between hydrogen and deuterium plasmas. In both cases, clear type-I ELMs are observed while the ELM frequency for the hydrogen plasma of $f_{ELM} \sim 150$ Hz is higher than that for the deuterium plasma of $f_{ELM} \sim 55$ Hz. If Δ_{ped} varies in proportion to ρ_{pol}^* ($\propto m^{0.5}$), it would be impossible to match the pedestal height for both plasmas at the same edge pressure gradient. Hence, the similar edge T_i profiles between deuterium and hydrogen plasmas are indicative of a weak dependence of Δ_{ped} on ρ_{pol}^* .

In this series of experiments on the dimensionless parameter scan, we obtain the scaling of the H-mode transport barrier width. The log-linear regression analysis indicates the scaling expressed as $\Delta_{ped} = 0.315a\rho_{pol}^*{}^{0.2}\beta_{pol}{}^{0.5}$. Fig. 6(a) shows the comparison of Δ_{ped}/a with the scaling expression. In Fig. 6(a), in addition to the dimensionless parameter scan, the

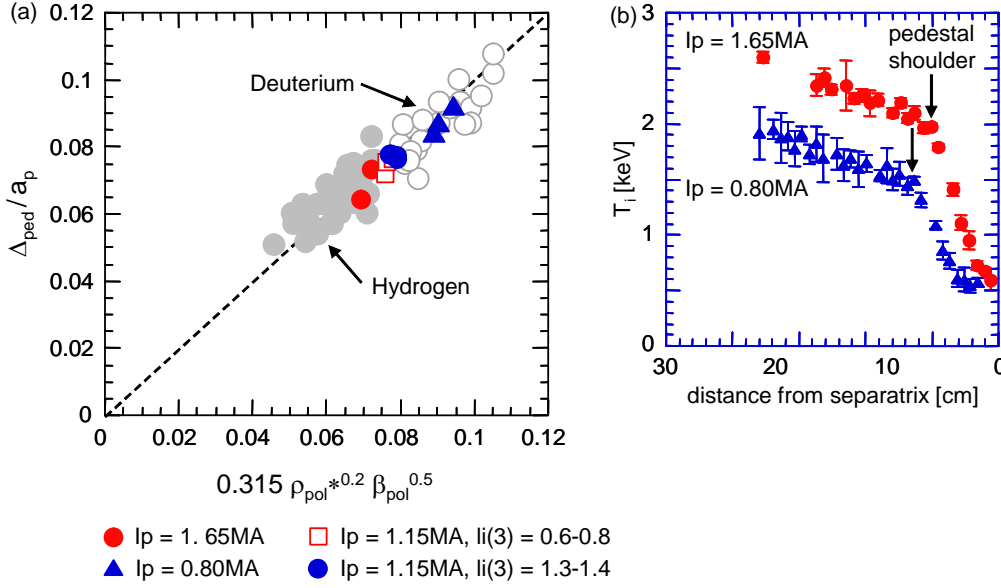


FIG. 6. (a) The comparison of Δ_{ped}/a with the scaling expression of $0.315\rho_{pol}^{*0.2}\beta_{pol}^{0.5}$ obtained through the dimensionless experiments using deuterium and hydrogen. (b) The edge T_i profiles for the cases of $I_p = 0.80MA$ and $1.65MA$ operated in the standard current density profile at $l_i \sim 1$, where the averaged boundary B_p values are $1.2T$ and $3.1T$, respectively.

pedestal data in the I_p ramp experiments are also plotted. As shown in Fig. 4, the pedestal density and temperature can vary by conducting I_p ramp up and down while the pedestal pressure remains almost constant at $I_p = 1.15MA$. In case where the edge density becomes lower in high l_i discharge, the pedestal temperature increases accompanied by a slight change in Δ_{ped} (see Fig. 4(c)). This change in Δ_{ped} can be expressed by the weak ρ^*_{pol} dependence in the scaling at almost constant β_{pol} . As shown in Fig. 6(a), the spatial width of the H-mode pedestal obtained in the I_p ramp experiment follows the scaling. In fact, since the edge current density profiles are not accurately measured, it is hard to evaluate quantitatively the effect of the edge magnetic shear on the pedestal width. Considering that the variation of the pedestal width obtained by I_p ramp remains in the range where the data is not largely deviated from the evaluated scaling using ρ^*_{pol} and β_{pol} , the effect of the edge magnetic shear on the pedestal structure might not be large. Fig. 6(b) shows the edge T_i profiles for the cases of $I_p = 0.80MA$ and $1.65MA$ operated in the standard current density profile at $l_i \sim 1$, where the boundary B_p values are $1.2T$ and $3.1T$, respectively. Then, $T_i^{ped} \sim 1.5keV$ and $\sim 2.0keV$ are obtained at $0.80MA$ and $1.65MA$, respectively. Since the pedestal pressure depends on the plasma current as $p_{ped} \propto I_p^{-1-1.5}$, the $\beta_{pol} (\propto nT/I_p^2)$ at the pedestal tends to decrease with I_p . As shown in Fig. 6(b), Δ_{ped} shrinks with decreasing β_{pol} at high $I_p (=1.65MA)$. This I_p scan data are also plotted in Fig. 6(a). One can find that the change in Δ_{ped} due to the variation of I_p or the edge B_p value follows the scaling through the changes in ρ^*_{pol} and β_{pol} .

5. Summary

In this study, conducting the I_p ramp experiments in JT-60U, the heat transport and edge pedestal structure in the variation of the current ramp up and down discharges are examined. In addition, focusing on the poloidal dimensionless parameters in the poloidal system determined by I_p , the dependence of Δ_{ped} on ρ^*_{pol} and β_{pol} is examined by conducting dedicated mass scan experiments using hydrogen and deuterium plasmas.

Higher energy confinement is obtained in higher l_i H-mode. The profiles of the core

electron density and electron temperature are tends to be peaked. The H-factor evaluated for the core plasma of H-mode ($H_{89\text{core}}$) depends strongly on l_i with the relation of $H_{89\text{core}} \propto l_i^{0.77}$ in case of $l_i < 1$. However, at $l_i > 1$, the existence of strong sawtooth prevents from the increase of the core H-factor at higher l_i regime ($H_{89\text{core}} \sim 1.5$ at $l_i > 1$). This tendency is also seen in the case of L-mode plasmas. In order to evaluate the level of the achievable temperature gradient depending on the current density profile, the power scan was conducted. It is found at higher l_i that larger W_{th} is obtained at a given P_{abs} . On the other hand, no clear difference in W_{ped} is observed between the cases of high and low l_i plasmas. Thus, the increase of W_{th} at higher l_i is attributed mainly to the energy confinement improvement in the core plasma. The changes in χ_i in the power scan are similar between the low and high l_i cases. On the contrary to the ions, dT_e/dr becomes stronger at a given heat flux, resulting in the reduction in χ_e . A clear difference is observed in ELM activity. The ELM frequency f_{ELM} at higher l_i becomes higher at a given P_{sep} . The edge pedestal pressure is not significantly changed by the I_p ramp technique. However, higher l_i H-mode tends to have relatively lower pedestal density. Thus, in the case of higher l_i plasma, higher pedestal temperature can be obtained by the reduced edge density.

While a variety of empirical scalings of Δ_{ped} in the H-mode plasmas have been proposed, these scalings vary from machine to machine, in which ρ^*_{pol} and β_{pol} are intermingled. This disagreement of the scalings can be caused by a existing strong link between ρ^*_{pol} and β_{pol} . To distinguish these variables, a pair of experiments in hydrogen and deuterium plasmas are conducted. An explicit difference between ρ^*_{pol} and β_{pol} is the mass dependence of ρ^*_{pol} ($\propto m^{0.5}$) in contrast to no mass dependence in β_{pol} . Then, the ρ^*_{pol} at the H-mode edge pedestal is not fixed but differs by the factor of ~ 1.4 (which is the square root of the mass ratio) while β_{pol} and v^* are almost the same. In this comparison, the similar edge T_i profiles are obtained between deuterium and hydrogen plasmas. This result is indicative of a weak dependence of Δ_{ped} on ρ^*_{pol} . In this series of experiments on the dimensionless parameter scan, we obtain the scaling of the H-mode transport barrier width expressed as $\Delta_{\text{ped}} = 0.315a\rho^*_{\text{pol}}{}^{0.2}\beta_{\text{pol}}{}^{0.5}$. This change in Δ_{ped} observed in the I_p ramp experiments also follows this scaling.

References

- [1] URANO, H., et al., Nucl. Fusion **42**, 76 (2002).
- [2] KAMADA, Y., et al., Nucl. Fusion **33**, 225 (1993).
- [3] OSBORNE, T. H., et al., Plasma Phys. Control. Fusion **40**, 845 (1998).
- [4] LINGERTAT, J., et al., Nucl. Mater. **266-269**, 124 (1999).
- [5] KAMADA, Y., et al., Plasma Phys. Control. Fusion **41**, 1371 (1999).
- [6] HATAE, T., et al., Plasma Phys. Control. Fusion **42**, A283 (2000).
- [7] URANO, H., et al., Nucl. Fusion **48**, 045008 (2008).